

Identifying topological-band insulator transitions in silicene and other 2D gapped Dirac materials by means of Rényi-Wehrl entropy

M. Calixto

*Departamento de Matemática Aplicada, Universidad de Granada,
Fuentenueva s/n, 18071 Granada, Spain*

E. Romera

*Departamento de Física Atómica, Molecular y Nuclear and
Instituto Carlos I de Física Teórica y Computacional,
Universidad de Granada, Fuentenueva s/n, 18071 Granada, Spain*

Abstract

We propose a new method to identify transitions from a topological insulator to a band insulator in silicene (the silicon equivalent of graphene) in the presence of perpendicular magnetic and electric fields, by using the Rényi-Wehrl entropy of the quantum state in phase space. Electron-hole entropies display an inversion/crossing behavior at the charge neutrality point for any Landau level, and the combined entropy of particles plus holes turns out to be maximum at this critical point. The result is interpreted in terms of delocalization of the quantum state in phase space. The entropic description presented in this work will be valid in general 2D gapped Dirac materials, with a strong intrinsic spin-orbit interaction, isostructural with silicene.

PACS numbers: 03.65.Vf, 03.65.Pm, 05.30.Rt,

I. INTRODUCTION

Silicene is a two dimensional crystal of silicon which has been studied theoretically [1, 2] and recently experimentally [3–7]. The low energy electronic properties can be described by a Dirac Hamiltonian, like in graphene, but the electrons are massive due to a relative large spin-orbit coupling Δ_{so} . In fact, silicene has a band gap $|\Delta_{s\xi}|$ (s and ξ denote spin and valley, respectively) which can be controlled by applying a perpendicular electric field $\mathcal{E}_z = \Delta_z/l$ (l is the interlattice distance of the buckled honeycomb structure) to the silicene sheet (see 1 for a plot of the band gap). It has been demonstrated [8] that there is a quantum phase transition, from a topological insulator (TI, $|\Delta_z| < \Delta_{\text{so}}$) to a band insulator (BI, $|\Delta_z| > \Delta_{\text{so}}$), at a charge neutrality point (CNP) $\Delta_z^{(0)} = s\xi\Delta_{\text{so}}$, where there is a gap cancellation between the perpendicular electric field and the spin-orbit coupling, thus exhibiting a semimetal behavior.

A 2D topological insulator is also known as a quantum spin Hall state, and it was theoretically studied in [9] and first discovered in HgTe quantum wells in [10]. The common characteristic of a TI-BI transition is a band inversion with a level crossing at some critical value of a control parameter (electric field, quantum well thickness, etc). In this paper we find that electron-hole entropies of a quantum state (in a phase-space representation) also exhibit this crossing/inversion behavior at the CNP, thus providing a new characterization of the TI-BI quantum phase transition (QPT).

The study of phase space properties in quantum systems can be done by using the Husimi function of a quantum state $|\psi\rangle$, which is defined as the squared overlap between a minimal uncertainty (coherent) state $|\alpha\rangle$ and $|\psi\rangle$, thus giving the probability of finding the quantum system in a coherent state. Husimi quasiprobability distribution has been useful for a phase-space analysis of metal-insulator transition [11], for the study of quantum chaos in physics [12], and recently in the analysis of QPTs in algebraic models [13–16]. Rényi-Wehrl entropies of the Husimi function (see section III for a definition) have been proved to be a good marker for QPTs of some paradigmatic models like: Dicke model [13] of atom-field interactions (undergoing a QPT from normal to superradiant), vibron model [14] for triatomic molecules (undergoing a shape QPT from linear to bent) and Lipkin-Meshkov-Glick model [15] used for example in nuclear physics and quantum optics. Rényi-Wehrl entropy displays either an extreme, or an abrupt change, at the critical point and therefore provides a detector of

QPTs across the phase diagram of a critical system.

In this work we shall analyze the topological-band insulator transition in silicene by using these phase-space techniques. The paper is organized as follows. Firstly, in Section II, we shall remind the low energy Hamiltonian for silicene, its eigenvectors and eigenvalues. Then, in Section III, we will define the Husimi function in this model and the Rényi-Wehrl entropies of the Husimi function. In Section IV we will show that the Rényi-Wehrl entropy turns out to be a clear marker of topological-band insulator transitions in silicene. Finally, some concluding remarks will be given in the last Section.

II. LOW ENERGY HAMILTONIAN

Let us consider a monolayer silicene with external magnetic B and electric \mathcal{E}_z fields applied perpendicular to the sheet. The effective low energy Hamiltonian is given by [8]

$$H_s^\xi = v_F(\sigma_x p_x - \xi \sigma_y p_y) - \xi s \Delta_{\text{so}} \sigma_z + \Delta_z \sigma_z, \quad (1)$$

where ξ corresponds to the inequivalent corners K ($\xi = 1$) and K' ($\xi = -1$) of the Brillouin zone, respectively, σ_j are the usual Pauli matrices, $v_F = 5 \times 10^5$ m/s is the Fermi velocity of the Dirac fermions (with up and down spin values being represented by $s = \pm 1$, respectively) and Δ_{so} is the band gap induced by intrinsic spin-orbit interaction, which provides a mass to the Dirac fermions. The spin-orbit energy gap induced by intrinsic spin-orbit coupling has been estimated (using density functional theory and tight-binding calculations [17–19]) as $\Delta_{\text{so}} \approx 1.55 - 7.9$ meV, and we will consider $\Delta_{\text{so}} = 4$ meV along this paper. The application of an external constant electric field \mathcal{E}_z creates an potential difference $\Delta_z = l\mathcal{E}_z$, with $l \simeq 0.23\text{\AA}$, between sublattices yielding a tunable band gap. See Figure 1 for a graphical representation.

Using the Landau gauge, $\vec{A} = (0, Bx, 0)$, and doing the minimal coupling $\vec{p} \rightarrow \vec{p} + \frac{e}{c}\vec{A}$ for the momentum, one can easily diagonalize the Hamiltonian (1) with eigenvalues [8, 20]

$$E_n^{s\xi} = \begin{cases} \text{sgn}(n)\sqrt{|n|\hbar^2\omega^2 + \Delta_{s\xi}^2}, & n \neq 0, \\ -\xi\Delta_{s\xi}, & n = 0, \end{cases} \quad (2)$$

in terms of the Landau level index $n = 0, \pm 1, \pm 2, \dots$, the cyclotron frequency $\omega = v_F\sqrt{2eB/\hbar}$ and the lowest band gap $\Delta_{s\xi} \equiv (\Delta_z - s\xi\Delta_{\text{so}})/2$. The corresponding eigenvectors

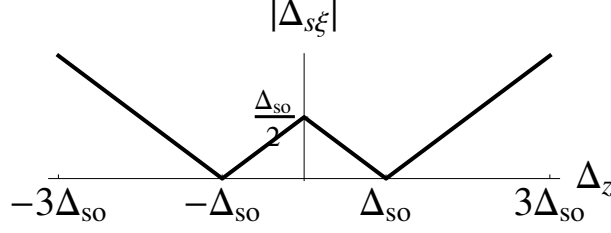


FIG. 1: The band gap $\Delta_{s\xi} = (\Delta_z - s\xi\Delta_{so})/2$ as a function of the electric potential Δ_z created by the perpendicular electric field applied to the silicene sheet. Δ_{so} is the spin-orbit energy gap induced by the intrinsic spin-orbit.

for the K and K' points are

$$|n\rangle_{s\xi} = \begin{pmatrix} -iA_n^{s\xi}||n| - (1 + \xi)/2\rangle \\ B_n^{s\xi}||n| - (1 - \xi)/2\rangle \end{pmatrix}, \quad (3)$$

where the constants $A_n^{s\xi}$ and $B_n^{s\xi}$ are given by [20]

$$A_n^{s\xi} = \begin{cases} \text{sgn}(n)\sqrt{\frac{|E_n^{s\xi}| + \text{sgn}(n)\Delta_{s\xi}}{2|E_n^{s\xi}|}}, & n \neq 0, \\ (1 - \xi)/2, & n = 0, \end{cases}$$

$$B_n^{s\xi} = \begin{cases} \sqrt{\frac{|E_n^{s\xi}| - \text{sgn}(n)\Delta_{s\xi}}{2|E_n^{s\xi}|}}, & n \neq 0, \\ (1 + \xi)/2, & n = 0, \end{cases} \quad (4)$$

and $||n\rangle$ denotes an orthonormal Fock state of the harmonic oscillator.

In Figure 2 we represent the low energy spectra given by eq. (2), as a function of the external electric potential Δ_z for $B = 0.5$ T (where T is the unit symbol for Tesla). The transitions TI-BI occur at the critical points $\Delta_z = s\xi\Delta_{so}$, where there is a band inversion for the $n = 0$ Landau level (either for spin up and down) at both valleys. The energies $E_0^{1,\xi}$ and $E_0^{-1,\xi}$ have the same sign in the BI phase ($|\Delta_z| > \Delta_{so}$, in blue), and different sign in the TI phase ($|\Delta_z| < \Delta_{so}$, in pink).

III. INVERSE PARTICIPATION RATIO AND RÉNYI-WEHRL ENTROPY

The standard canonical (or Glauber) coherent states for the 1D quantum harmonic oscillator are given by

$$|\alpha\rangle = e^{-|\alpha|^2/2}e^{\alpha a^\dagger}|0\rangle = e^{-|\alpha|^2/2}\sum_{n=0}^{\infty}\frac{\alpha^n}{\sqrt{n!}}|n\rangle, \quad (5)$$

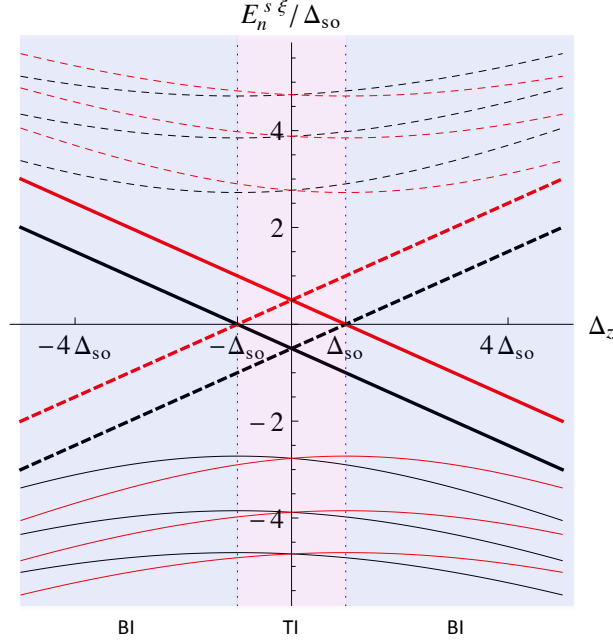


FIG. 2: Low energy spectra of silicene as a function of the external electric potential Δ_z for $B = 0.5$ T. Landau levels $n = \pm 1, \pm 2$ and ± 3 , at valley $\xi = 1$, are represented by dashed (electrons) and solid (holes) thin lines, black for $s = -1$ and red for $s = 1$ (for the other valley we simply have $E_n^{s,-\xi} = E_n^{-s,\xi}$). The lowest Landau level $n = 0$ is represented by thick lines at both valleys: solid at $\xi = 1$ and dashed at $\xi = -1$. Vertical blue dotted grid lines indicate the CNPs separating BI (blue) from TI (pink) phases.

with $\alpha \in \mathbb{C}$ (the phase space). The coherent states form an overcomplete set of the corresponding Hilbert space and verify the closure relation:

$$1 = \int_{\mathbb{R}^2} |\alpha\rangle \langle \alpha| \frac{d^2\alpha}{\pi}, \quad (6)$$

with $d^2\alpha = d\text{Re}(\alpha)d\text{Im}(\alpha)$. Using the coherent state (Bargmann) representation, we can associate a quasiprobability distribution (the so called Husimi function) $Q_\psi(\alpha) \equiv |\langle \alpha | \psi \rangle|^2$ to every normalized harmonic oscillator state $|\psi\rangle$. This definition is straightforwardly extended to any density matrix ρ as $Q_\rho(\alpha) = \langle \alpha | \rho | \alpha \rangle$. For example, the Husimi function of a Fock state $|n\rangle$ is simply

$$Q_n(\alpha) = |\langle n | \alpha \rangle|^2 = \frac{e^{-|\alpha|^2}}{n!} |\alpha|^{2n}. \quad (7)$$

Coherent states are said to be “quasi-classical” because of their minimum uncertainty (and dynamical) properties. To quantify the spread/localization of a wave packet ψ in phase

space, the ν -th moments of the corresponding Husimi function Q_ψ , defined by

$$M_\psi^\nu = \int_{\mathbb{R}^2} \frac{d^2\alpha}{\pi} (Q_\psi(\alpha))^\nu, \quad (8)$$

are often used. Note that, using (6), we have $M_\psi^1 = 1$ for normalized ψ . We shall focus on the $\nu = 2$ moment, also called the inverse participation ratio, which is related to the inverse area in phase space occupied by the Husimi function. Namely, for a Fock state $|n\rangle$ we have

$$M_n^2 = \frac{(2n)!}{2^{2n+1}(n!)^2}, \quad (9)$$

which is maximum for $n = 0$, $M_0^2 = 1/2$ (minimum area). Instead of the momentum M_ψ^ν , we shall use the Rényi-Wehrl entropy $W_\psi^\nu = \frac{1}{1-\nu} \ln(M_\psi^\nu)$ for the sake of convenience. Note that, for $\nu \rightarrow 1$, the previous expression reads $W_\psi^1 = -\int Q_\psi(\alpha) \ln(Q_\psi(\alpha)) d^2\alpha/\pi$, the so called Wehrl entropy. As conjectured by Wehrl [21] and proved by Lieb [22], any Glauber coherent state $|\alpha'\rangle$ has a minimum Wehrl entropy of $W_{\alpha'}^1 = 1$. We shall use $\nu = 2$, for which the minimum Rényi-Wehrl entropy is $W_{\min}^2 = \ln(2)$, corresponding to a coherent state.

IV. RÉNYI-WEHRL ENTROPY AS A MARKER OF TOPOLOGICAL-BAND INSULATOR TRANSITIONS

Now, we shall calculate the Rényi-Wehrl entropy W_n^2 of a Hamiltonian eigenstate (3) as a function of the electric potential Δ_z in order to analyze the TI-BI transition. We shall restrict ourselves to the valley $\xi = 1$, omitting this index from (3) and (4). All the results for $\xi = 1$ are straightforwardly translated to $\xi = -1$ by swapping electrons for holes (i.e., $n \leftrightarrow -n$) and spin up for down (i.e., $s \leftrightarrow -s$). Taking into account equations (3) and (7), we can write the expression of the Husimi function of a Hamiltonian eigenstate $|n\rangle_s$ as

$$Q_n^s(\alpha) = |\langle \alpha | n \rangle_s|^2 = (A_n^s)^2 Q_{|n|-1}(\alpha) + (B_n^s)^2 Q_{|n|}(\alpha), \quad (10)$$

and the second moment as

$$\begin{aligned} M_n^{2,s} &= (A_n^s)^4 M_{|n|-1}^2 + (B_n^s)^2 M_{|n|}^2 \\ &\quad + 2(A_n^s B_n^s)^2 \frac{(2|n| - 1)!}{4^{|n|} |n|! (|n| - 1)!} \end{aligned} \quad (11)$$

where we are using (9) and the value of $\int \frac{d^2\alpha}{\pi} Q_{|n|}(\alpha) Q_{|n|-1}(\alpha)$. For the sake of convenience, we shall use the Rényi-Wehrl entropy $W_n^{2,s} = -\ln(M_n^{2,s})$ to make graphical representations

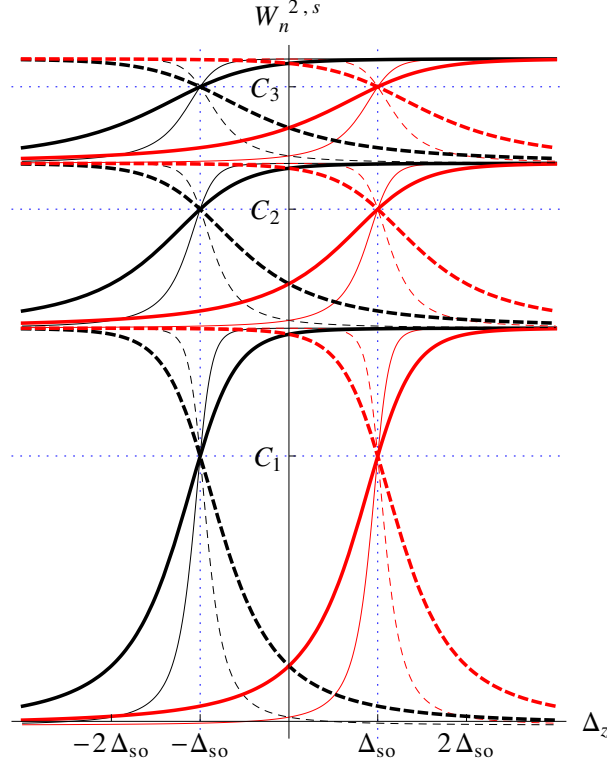


FIG. 3: Rényi-Wehrl entropy $W_n^{2,s}$ of a Hamiltonian eigenstate $|n\rangle_{s\xi}$ as a function of the electric potential Δ_z for the Landau levels: $n = 1, 2$ and 3 (electrons; dashed curves) and $n = -1, -2$ and -3 (holes; solid curves) and valley $\xi = 1$. Black and red curves correspond to spin $s = -1$ and $s = 1$, respectively. Electron and hole entropy curves cross (“entropy inversion”) at the critical value of the electric potential $\Delta_z^{(0)} = -s\Delta_{so}$ (vertical blue dotted grid lines indicate this CNPs), with crossing entropy values denoted by $C_n = W_n^{2,s}(\Delta_z^{(0)})$, $n = 1, 2, 3$ and given in equation (12) (horizontal blue dotted grid lines indicate these crossing points). Thin and thick lines correspond to magnetic fields $B = 10^{-3}$ and $B = 10^{-2}$ T, respectively.

as a function of Δ_z for different values of the Landau level n , spin $s = \pm 1$ and the magnetic field B . In Figure 3 we plot $W_n^{2,s}$ as a function of Δ_z for $n = 1, 2, 3$ (electrons) and $n = -1, -2, -3$ (holes) with spin up $s = 1$ (in red) and down $s = -1$ (in black). Entropy for holes ($n < 0$, solid curves) is an increasing function of the electric potential Δ_z , whereas entropy for electrons ($n > 0$, dashed curves) is a decreasing function of Δ_z . Electron-hole entropy curves cross at the CNP $\Delta_z^{(0)} = -s\Delta_{so}$, where the entropy is

$$C_n \equiv W_n^{2,s}(\Delta_z^{(0)}) = -\ln \left(\frac{(8|n| - 3)\Gamma(|n| - \frac{1}{2})}{16\sqrt{\pi}\Gamma(|n| + 1)} \right). \quad (12)$$

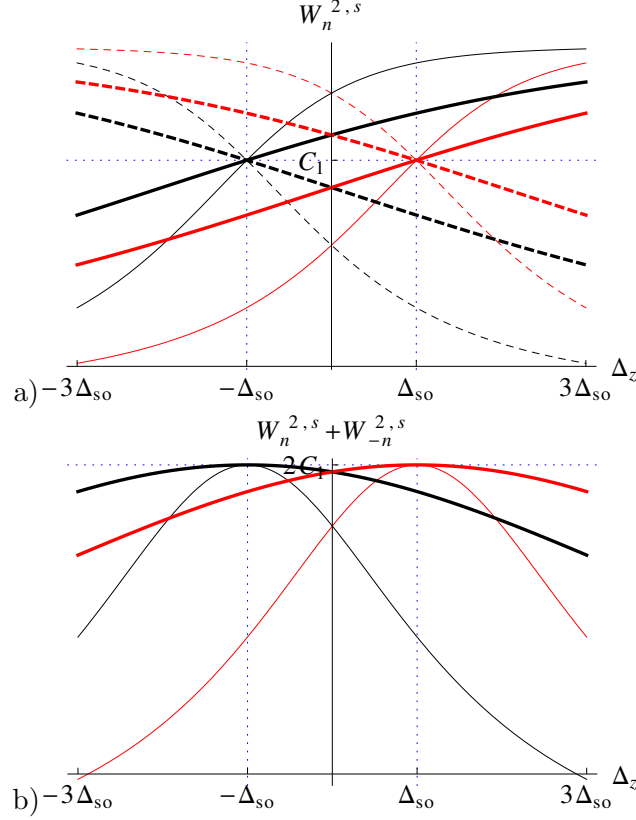


FIG. 4: a) Same representation as in Figure 3 but for $n = \pm 1$ only and magnetic fields $B = 0.1$ (thin) and $B = 1$ T (thick), respectively. b) Combined entropy $W_n^{2,s} + W_{-n}^{2,s}$ of electrons plus holes for $n = 1$. The entropy of the electron-hole compound exhibits a maximum of $2C_n$ at the CNP $\Delta_z^{(0)} = -s\Delta_{so}$.

Note that the critical entropy (12) only depends on the Landau level n (and not on other physical magnitudes like: B, v_F, e, s , etc) thus providing a universal characterization of the topological-band insulator QPT, which is shared with other two-dimensional crystals like Ge, Sn and Pb. Indeed, in Figure 3 we plot entropy for magnetic field $B = 10^{-2}$ (thick lines) and $B = 10^{-3}$ T (thin lines) and note that entropy slopes at $\Delta_z^{(0)}$ decrease with B but they have a common critical entropy (12). For electrons (holes), minimum (maximum) entropies for a given Landau level n are attained at asymptotic values $\Delta_z \rightarrow \infty$, and maximum (minimum) entropies are attained at $\Delta_z \rightarrow -\infty$. The minimum and maximum entropies

turn out to depend only on $|n|$ as

$$\begin{aligned} W_{n,\min}^{2,s} &= -\ln \left(\frac{|n|\Gamma(|n| - \frac{1}{2})}{2\sqrt{\pi}\Gamma(|n| + 1)} \right) \\ W_{n,\max}^{2,s} &= -\ln \left(\frac{(|n| - \frac{1}{2})\Gamma(|n| - \frac{1}{2})}{2\sqrt{\pi}\Gamma(|n| + 1)} \right), \end{aligned} \quad (13)$$

where Γ denotes the usual gamma function. Note that $W_{n+1,\min}^{2,s} = W_{n,\max}^{2,s}$, as can also be seen in Figure 3. For example, $W_{\pm 1,\min}^{2,s} = \ln(2)$ (which means that the Hamiltonian eigenstate $|\pm 1\rangle_s$ is a coherent state of electrons for $\Delta_z \rightarrow \infty$ and a coherent state of holes for $\Delta_z \rightarrow -\infty$) and $W_{\pm 1,\max}^{2,s} = 2\ln(2)$ (which means that $|\pm 1\rangle_s$ is a “cat state” of electrons for $\Delta_z \rightarrow -\infty$ and a cat state of holes for $\Delta_z \rightarrow \infty$). Indeed, as commented after (9), the minimum entropy of $W_{\min}^2 = \ln(2)$ is attained for coherent states. The so-called “cat states” arise in many models undergoing a QPT (see e.g., [13–15]) and are a superposition of two coherent (semiclassical) states with negligible overlap, so that their entropy is twice the minimum entropy, that is, $2\ln(2)$.

In Figure 4 we plot the case $n = \pm 1$ for higher magnetic fields ($B = 0.1$ and $B = 1$ T in panel a) and the combined entropy of electrons plus holes, $W_n^{2,s} + W_{-n}^{2,s}$ (in panel b), which exhibits a maximum of $2C_n$ at the CNPs. For $n = \pm 1$, the maximum entropy of the electron-hole compound is $2C_1 = 2\ln(16/5) \simeq 2.3263$ (see Figure 4, panel b). The asymptotic behavior of the maximum combined entropy for large n is $2C_n \simeq \ln(4\pi) + \ln(|n|) + O(1/|n|)^{3/2}$, which shows an increasing logarithmic behavior with $|n|$.

The existence of a maximum electron plus hole entropy means that the combined wave function spreads across the phase space, taking up a bigger volume (it is more delocalized) at the CNP. In Figure 5 we also plot the combined renormalized entropy

$$\overline{W}_{\pm n}^{2,s} = W_n^{2,s} + W_{-n}^{2,s} - W_{n,\min}^{2,s} - W_{n,\max}^{2,s} \quad (14)$$

of particles plus holes for $n = 1$ (solid lines) and $n = 2$ (dashed lines) together. We see that entropy “hats” become flatter and flatter as n increases.

The global behavior of the entropies $W_n^{2,s}$, as a function of the electric field strength, exhibits some common features with the band inversion behavior for the $n = 0$ Landau level (see Fig. 2 and comments at the end of Section II). Indeed, defining the renormalized entropy

$$\widetilde{W}_n^{2,s}(\Delta_z) = W_n^{2,s}(\Delta_z) - C_n = -\ln \left(\frac{M_n^{2,s}(\Delta_z)}{M_n^{2,s}(\Delta_z^{(0)})} \right), \quad (15)$$

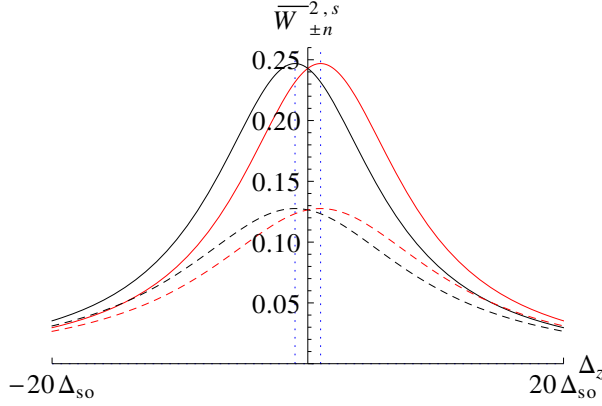


FIG. 5: Renormalized Rényi-Wehrl entropies (14) of the electron-hole compound for a Hamiltonian eigenstate $|n\rangle_{\xi,s}$ as a function of the electric potential Δ_z ($B = 1$ T) for the Landau levels $n = 1$ (solid lines) and $n = 2$ (dashed lines), and valley $\xi = 1$. Black and red curves correspond to spin $s = -1$ and $s = 1$, respectively. Vertical blue lines indicate the CNPs.

one can see that the quantities $\widetilde{W}_n^{2,s}(\Delta_z)$ and $\widetilde{W}_n^{2,-s}(\Delta_z)$ (for $n = \pm 1, \pm 2, \dots$) have the same sign in the BI phase ($|\Delta_z| > \Delta_{so}$), and different sign in the TI phase ($|\Delta_z| < \Delta_{so}$). See e.g. Figure 4 for $B = 1$ T (thick lines). Therefore, this “entropy-inversion” provides a clear characterization of each phase.

Additionally, taking into account that $\widetilde{W}_n^{2,s}$ measures the area occupied by the eigenstate $|n\rangle_s$ in phase space, we can say that, in the BI phase, an spreading (resp. localization) effect can be observed in the electrons (resp. holes) for $\Delta_z < -\Delta_{so}$ and in the holes (resp. electrons) for $\Delta_z > \Delta_{so}$; in the TI phase there is a spreading effect in the electrons with spin up and holes with spin down, and a localization in electrons with spin down and holes with spin up. We observe that the lower the magnetic field strength, the sharper these spreading and localization effects are.

V. CONCLUSIONS

In this work we have shown that the Husimi function is an appropriate tool to study topological-band insulator transitions in silicene and other gapped isostructural Dirac materials with intrinsic spin-orbit coupling as germanene, stantene or Pb. In particular, the Rényi-Wehrl entropy of the Husimi function of order two (related to the inverse participation ratio) has been used to analyze the TI to BI quantum phase transition, showing the

critical points of this transition clearly as a crossing/inversion behavior of the electron and hole entropies at the charge neutrality point. Critical (12) and asymptotic (13) values of electron-hole entropies only depend on the Landau level n , and not on any other physical quantities like: magnetic strength, Fermi velocity, electron charge, etc. Therefore, these entropic measures provide a universal characterization of the topological-band insulator QPT, which is shared with other two-dimensional crystals like Ge, Sn and Pb.

We want to emphasize that all the descriptions in terms of Rényi-Wehrl entropies that we have presented in this work will be valid in (isostructural) 2D gapped Dirac materials with a strong intrinsic spin-orbit interaction. Actually, all the characterizations studied here will apply to Ge, Sn and Pb counterparts. In fact, all the Figures will be valid by simply replacing the value of Δ_{so} in each case: $\Delta_{\text{so}}^{\text{Ge}} = 11.8$ meV for germanene, $\Delta_{\text{so}}^{\text{Sn}} = 36.0$ meV for stanene, $\Delta_{\text{so}}^{\text{Pb}} = 207.3$ meV for Pb [23]. Moreover, Dirac equation (and modifications) provides an effective model for a large family of topological insulators, and an entropic description like the one done in this letter could also shed new light on the better understanding of topological phases in these physical systems. This deserves a separated and more thorough study and it will be the subject of future work.

Acknowledgments

The work was supported by the Spanish Projects MICINN FIS2011-24149, CEIBIOTIC-UGR PV8, the Junta de Andalucía projects FQM.1861 and FQM-381.

-
- [1] K. Takeda, K. Shiraishi, Phys. Rev. B 50 (1994) 14916.
 - [2] G. G. Guzman-Verri, L. Lew Yan, Phys. Rev. B 76 (2007) 075131.
 - [3] P. Vogt et al., Phys. Rev. Lett. 108 (2012) 155501.
 - [4] B. Augray, A. Kara, S. B. Vizzini, H. Oughaldou, C. LéAndri, B. Ealet, G. Le Lay, App. Phys. Lett. 96 (2010) 183102.
 - [5] B. Lalmi, H. Oughaddou, H. Enriquez, A. Kara, S. B. Vizzini, B. N. Ealet, B. Augray, App. Phys. Letters 97 (2010) 223109.
 - [6] A. Feurence, R. Friedlein, T. Ozaki, H. Kawai, Y. Wang, Y. Y. Takamura, Phys. Rev. Lett. 108 (2012) 245501.

- [7] P. E. Padova et al., App. Phys. Lett. **96** (2010) 261905.
- [8] M. Tahir, U. Schwingenschlögl, Scientific Reports, **3**, 1075 (2013).
- [9] Kane C L and Mele E J, Phys. Rev. Lett. **95**, 226801 (2005)
- [10] B. Andrei Bernevig, Taylor L. Hughes and Shou-Cheng Zhang, Science **314**, 1757-1761 (2006).
- [11] C. Aulbach, A. Wobst, G.-L. Ingold, P. Hanggi and I. Varga, New J. of Physics **6**, 70 (2004).
- [12] P. A. Dando and T. S. Monteiro, J. Phys. B. **27**, 2681, (1994).
- [13] E. Romera, R. del Real, M. Calixto, Phys. Rev. A **85**, 053831, (2012).
- [14] M. Calixto, R. del Real, E. Romera, Phys. Rev. A **86**, 032508 (2012).
- [15] E. Romera, M. Calixto and O. Castaños, Physica Scripta **89**, 095103 (2014)
- [16] M. Calixto, O. Castaños and E. Romera, EPL **108**, 47001 (2014).
- [17] N. D. Drummond, V. Zólyomi, and V. I. Fal'ko, Phys. Rev. B **85**, 075423 (2012).
- [18] C. C. Liu, W. Feng, and Y. Yao, Phys. Rev. Lett. **107**, 076802 (2011).
- [19] C. C. Liu, H. Jiang, and Y. Yao, Phys. Rev. B **84**, 195430 (2011).
- [20] L. Stille, C. J. Tabert, and E. J. Nicol, Phys. Rev. B **86**, 195405 (2012).
- [21] Wehrl A 1979 Rep. Math. Phys. **16** 353
- [22] Lieb E H 1978 Commun. Math. Phys. **62** 35
- [23] W-F. Tsai, C-Y. Huang, T-R Chang et al. Nat. Commun. **4**, 1500 (2013)